Ecological Modelling 510 (2025) 111339

Contents lists available at ScienceDirect

Ecological Modelling

journal homepage: www.elsevier.com/locate/ecolmodel

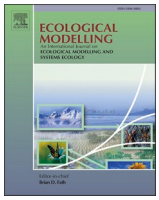

Are locally trained allometric functions of forest aboveground biomass universal across spatial scales and forest disturbance scenarios?

Benedikt Hartweg [a,*], Leonard Schulz [b], Andreas Huth [b], Konstantinos Papathanassiou [c], Lukas W. Lehnert [a]

[a] Department of Geography, Ludwig-Maximilians-Universität München, Munich, Germany
[b] Department Ecological Modelling, Helmholtz Centre for Environmental Research (UFZ), Leipzig, Germany
[c] German Aerospace Center e.V. (DLR), Wessling, Germany

ARTICLE INFO

Keywords:
Carbon cycle
Tropical forests
Biomass
Allometry
Scales
Forest height
Forest model

ABSTRACT

Large scale above-ground-biomass (AGB) estimation remains highly uncertain. Multi-sensor, multi-scale and multi-temporal analyses are crucial for capturing the dynamics and the heterogeneity of forests. The European Space Agency's BIOMASS mission will play a key role in future biomass monitoring. Considering the differences in the spatial scales of input datasets, it is essential to investigate these scale effects. This study examines whether locally trained allometric relationships between forest height and AGB are scale-dependent and how forest disturbances impact these estimates.

Using the forest gap model FORMIND, initialized with inventory data from tropical lowland forests close to Manaus (Brazil), we simulated forest height and AGB raster products at resolutions ranging from 20 m to 200 m based on various forest height metrics. Through regression analysis, allometric parameter sets for each resolution step were derived. We then tested the impact of applying these parameters under various conditions, including off-scale and off-scenario usage.

Our results show that applying allometric parameters at mismatched spatial scales introduces significant additional errors. This error becomes more prominent as scale differences increase. Additionally, the type and severity of forest degradation scenario strongly influences the estimation quality. However, dynamically adapting allometric parameter sets to local conditions mitigates these errors. Applying the locally trained parameters to varying disturbance scenarios results in substantial errors, underscoring the importance of incorporating local forest structure in AGB models.

While using off-scale allometric parameters is possible, it introduces additional challenges. Our study highlights the need for local forest structure products to improve large-scale AGB estimation.

1. Introduction

Estimates on the size of the global carbon potential and current stock in forests remain highly uncertain, despite its indisputable role for the climate system (Chave et al., 2005; Erb et al., 2018; Mo et al., 2023). In the meantime, disturbances in forest ecosystems are increasing in many parts of the world, but especially in tropical forests, thus accelerating the need for suitable estimates of carbon stocks over time, while considering local disturbance regimes (Lewis et al., 2015; Mo et al., 2023; Pan et al., 2013). To estimate carbon stocks, Aboveground Biomass (AGB) is frequently used as proxy, which is defined as the total amount of dry matter stored in living trees over ground. To date, in-situ measurements

Abbreviations: AGB, Above Ground Biomass; BGB, Below Ground Biomass; CH, Canopy Height; DBH, Diameter at Breast Height; DLR, German Space Agency; ESA, European Space Agency; FI, Field Inventories; FH, Forest Height; GEDI, Global Ecosystem Investigation; GFBI, Global Forest Biodiversity Initiative; IBGM, Individual-Based Forest Gap Model; InSAR, Interferometric SAR; ISS, International Space Station; KDE, Kernel Density Estimation; LAI, Leaf Area Index; LBA, Large Scale Biosphere-Atmosphere Experiment in Amazonia; LiDAR, Light Detection and Ranging; NASA, National Aeronautics and Space Administration; PFT, Plant Functional Type; PolSAR, polarimetric SAR; Pol-InSAR, polarimetric interferometric SAR; RMS, RMSE, Root Mean Square Error; RS, Remote Sensing; SAR, Synthetic Aperture Radar; SOC, Soil Organic Contents; SSR, Sum of Squared Residuals; TomoSAR, Tomographic SAR.

Changes to the original manuscript are marked in blue.

* Corresponding author.
E-mail address: ben.hartweg@lmu.de (B. Hartweg).

https://doi.org/10.1016/j.ecolmodel.2025.111339
Received 2 December 2024; Received in revised form 31 August 2025; Accepted 3 September 2025
Available online 24 September 2025

of forest Field Inventories (FI) represent the gold standard of forest structure analysis and non-destructive biomass and carbon quantification (Hetzer et al., 2020). Despite their essential role in AGB estimation of tropical forests, expanding FI data coverage remains a significant challenge.

Using FI data, AGB can be derived at an individual tree level through a function of the wood specific density ρ and the volume of the tree (simplified through the stem diameter and the tree height H). The tree's diameter D is commonly defined as the Diameter at Breast Height (130 cm, DBH) (Chave et al., 2019).

$$AGB = f(\rho, D, H) \tag{1}$$

Since ρ is considered, the formula is consistent across forest types, despite possible effects of regional or environmental changes (Chave et al., 2014). As species diversity, count of trees and blocked canopy line of sight can drastically increase the complexity of the estimation in very dense tropical forests, the above equation must be further abstracted to estimate AGB. For this, the *DBH* or the individual tree height H can be used, which is expected to follow a power law function with AGB (Mette, 2004).

$$AGB = \propto \times DBH^{\beta} \tag{2}$$

$$AGB = \propto \times H^{\beta} \tag{3}$$

The actual meaning behind the allometric factor α and the allometric exponent β is not consistently defined throughout the literature. Partly, α and β are seen as purely statistical parameters from the regression analysis of FI and Remote Sensing (RS) data (Saatchi et al., 2011), or they are attributed to a physical and ecological significance based on individual tree proportions, or forest stand properties. Again, the interpretation also depends on the observed scale. Observing individual trees, α is attributed to ρ, and β is seen as scaling exponent between either *DBH* or H and the AGB, partially correlating with the tree stage (Pilli et al., 2006; West et al., 1999; Zianis and Mencuccini, 2004).

By changing the scale from individual trees to forest stands, for obvious reasons the AGB estimation can no longer be achieved by the sum of the individual estimations. More aggregated parameters must be used to drive the allometric equations in (2) and (3). Despite recent advances to estimate DBH trough means of drone Light Detection and Ranging (LiDAR) systems (Neuville et al., 2021), these methods are still in their development phase and restricted to very specific forest types. Given that the Forest Height (FH) can be operationally mapped by means of waveform LiDAR (e.g. NASA GEDI), or Synthetic Aperture Radar (SAR) interferometry (DLR TerraSAR-X/TanDEM-X, ESA BIOMASS), the usage of the FH paves the way to apply Eq. (3) on considerably larger scales. Yet, the usage of such a highly aggregated and scale depended variable poses additional challenges (Köhler and Huth, 2010; Ni-Meister et al., 2022). On the stand scale, α may be attributed to anthropogenically or naturally induced changes in stand density (the number of trees per area unit), and β may be seen as a rough proxy for growing conditions and successional state (Choi et al., 2021). Despite the limited research in this direction of interpreting α and β, this opens the possibility to expand the AGB estimation model described in Eq. (3) and to create localized allometries, with FH as main predictor. Thus, for this study, Eq. (4) will be used throughout all analyses and research questions.

$$AGB_{stand} = \propto \times FH^{\beta} \tag{4}$$

A milestone towards creating reliable time-series estimates of large-scale tropical AGB will be provided by the BIOMASS mission of the European Space Agency (ESA) which launched on April 29, 2025. The mission will consist of a single P-Band, fully polarimetric, SAR satellite and will provide a polarimetric interferometric SAR (Pol-InSAR) coverage of forested areas in a 75° N to 56° S latitudinal band. Repetition times will be every seven months with a spatial resolution of 200 m × 200 m or 4 ha. In addition to the SAR data, the main outputs will consist of the AGB products at 4 ha resolution, a one-of-a-kind forest (canopy) height map at 4 ha resolution and a forest disturbance map for discrete classification into several disturbance regimes at 50 m × 50 m or 0.25 ha (Le Toan et al., 2011; Quegan et al., 2019). With the strong link between forest variables like FH and AGB, this FH product will enable the wide scale application of FH to AGB allometric models.

An obvious question of scale dependencies arises, when applying allometric models derived from FI data to an 4 ha resolution forest height map. Several studies were conducted investigating the relationship between different FH definitions and AGB at varying spatial scales (Armstrong et al., 2020; Köhler and Huth, 2010; Meyer et al., 2013). With increasing scale (decreasing spatial resolution), a reduction of precision and an increase of accuracy was observed in all three studies. High resolution scales are naturally better suited to describe the local forest structure, with estimates often influenced by the local distribution of the most prominent trees. On broader scales AGB estimates are considerably more accurate and spatially less variable, with the downside of a loss of information on the forest structure (Armstrong et al., 2020; Meyer et al., 2013). The question arises, whether these changes in the observed scale have actual effects on the estimation of AGB using FH to AGB allometric models.

To test scale-dependencies and to investigate effects of different disturbance regimes on the allometric functions, multivariate individual tree measurements and extensive and spatially vast FI datasets would be needed. Due to the inherent and obvious lack of such, simulations from the high resolution individual forest gap model FORMIND by the Helmholtz-Centre for Environmental Research UFZ (Rödig et al., 2017) will be utilized throughout this paper. Also, by applying Individual-Based Forest Gap Models (IBGM) such as FORMIND, different forest use and degradation scenarios (old-growth, alias natural, wildfires, logging) can be simulated and be accounted for in the analysis.

Given the future availability of a wide scale FH product from the ESA BIOMASS mission and the possibilities of AGB estimation from FH to AGB allometric models, the emphasis of this paper is to put a spotlight on the questions of the applicability of allometric biomass models across scales and forest disturbance regimes. Thus, the following lead research questions are defined (Q1 to Q3):

(I) How do the statistical relationship and the allometric parameters between FH and ABG change with scale?
(II) Can a set of allometric parameters be applied to a vastly different and considerably coarser resolution scale (e.g. GEDI derived parameters and BIOMASS FH map)? How much error would be introduced by doing so? Could the additional error be compensated by using estimates of α at the corresponding scale?
(III) What is the effect of not knowing the disturbance state of the forest? For example, how does the AGB estimation perform, if sets of allometric parameters from disturbed regimes are applied to late-successional undisturbed forests patches?

2. Materials and methods

2.1. The FORMIND model

To establish allometric functions for different disturbance regimes and spatial scales, simulations from the high resolution IBGM FORMIND by the Helmholtz-Centre for Environmental Research UFZ (Rödig et al., 2018) have been utilized. FORMIND has specifically been developed to simulate tropical forests. Apart from completely simulating tree growth, mortality, competition and recruitment at user defined scales, it features three key characteristics that provide a unique opportunity for our research: (1) it drastically reduces the species complexity of tropical forests by grouping tree species with similar attributes into Plant Functional Types (PFT), thus reducing model uncertainty concerning species and facilitating model parametrization; (2) both natural and

anthropogenic disturbances are modelled, with their respective effects on forest structure and forest dynamics; (3) the carbon balance and biomass assimilation are simulated on the scale of individual trees with a detailed process-based approach (Armstrong et al., 2020; Fischer et al., 2016; Rödig et al., 2017). Fig. 1 shows the basic concept of the FORMIND IBGM. The main inputs are light (global radiation, photosynthetic photon flux density) and the grouping and parametrisation of the PFT. For every processing year, establishment, competition, growth and mortality are simulated and projected onto the individual tree carbon balance (Rödig et al., 2017).

Another key concept inherent to IBGM is the usage of forest gaps. In the case of FORMIND, the simulated area is segmented into 20 m × 20 m patches, roughly matching the size of gaps caused by falling trees. These patches interact in seed dispersal and the falling of large trees, thus the simulated forests represent a collection of these patches at different successional stages. Given this concept, the patch size fraction equals the smallest possible spatial resolution for rasterized datasets, apart from looking at the simulation results on the scale of individual trees (Armstrong et al., 2020; Fischer et al., 2016; Rödig et al., 2017).

2.2. Model initialization

The FORMIND simulation used in this analysis is based on the initialization and parametrization settings described in Rödig et al., 2017 and Rödig et al., 2018. 25 ha of Brazilian central Amazon basin tropical rainforest were simulated for 1000 years (1 year time step), under different environmental and anthropogenic use scenarios. The simulation started from bare earth. FI data from the Large Scale Biosphere-Atmosphere Experiment Amazonia (LBA) (Brondizio et al., 2009) and studies by Kunert et al., 2015 in Brazil were used for the classification of the trees into PFTs and the calibration of the model. The undisturbed simulation used in this article is based on an old growth tropical lowland forest near Manaus (02°38′22.54″S 60°09′51.34″W). Tree species diversity is estimated with 250 species per ha (Kunert et al., 2015). This tree species richness was aggregated into three PFTs, which are abstracted according to the mean wood density, which is a proxy of growth and successional characteristics and thus the forest dynamics (Chave et al., 2006). Tree species with a density (expressed as organic dry matter) below 0.45 t / m^3 are allocated to PFT 1, between 0.45 t / m^3 and 0.55 t / m^3 to PFT 2 and above 0.45 t / m^3 to PFT 3 (Kazmierczak et al., 2014; Rödig et al., 2017).

PFT 1 represents fast growing, pioneering vegetation, that is dependent on high light availability thus having relatively low wood densities. PFT 2 contains an intermediate successional state with semi fast-growing species and higher wood densities. PFT 3 stands for slow-growing trees with high wood densities and the comparatively highest shade tolerance. This group represents trees of an old-growth late successional forest (Rödig et al., 2017).

Forest succession is driven by mortality, photosynthesis and minimum light availability. Parametrization for the respective function was performed by numeric calibration against the mentioned forest inventories at varying successional stages. A match between simulated and observed values for Leaf Area Index (LAI), biomass and tree diameter distributions was observed (Fischer et al., 2016; Rödig et al., 2017).

To investigate the effect of disturbances on allometric functions, three model cases were assessed for the analysis. First, the natural scenario represents a non-disturbed forest, where the dynamic is partly influenced by the mortality of large trees within PFT 3 creating gaps. Second, the logging scenario is characterized by a semi-stochastic process, by which trees with DBH of up to 1.5 m are subjected to logging events and cause destruction to their surrounding trees by falling. A more detailed representation of the FORMIND logging process can be found in Huth et al., 2005. This damage is influence by the applied logging strategy (here: high impact conventional logging) at a logging interval of 50 years. The third disturbance regime consists of wildfires. For every simulation year, a random number of fire events are triggered following a mean fire frequency per ha (25 fires / ha), a mean fire size (0.6 ha) and a mean fire severity (0.6, with 0 being low and 1 being max). The spread of the fire to neighbouring patches is modelled randomly (Fischer, 2021; Fischer et al., 2016; Huth et al., 2005).

Fig. 2 depicts the AGB dynamics of the 3 scenarios over the 1000-year timespan and forms the data basis for the following analysis (area size 25 ha). Mean AGB values are indicated in t / ha, with the shaded areas representing the 90 % confidence interval, thus the spatial variation across the 25 individual 1 ha cells.

2.3. FORMIND rasterization

As mentioned, FORMIND provides data on each individual tree within the 25 ha plot for each time step. To proceed with our analysis, this individual tree data needs to be rasterised at the defined spatial resolution scales. FH is the main predictor in the allometric model used in this analysis (see Eq. (4)). We used four commonly applied FH definitions to generate the respective raster products and compare the results. In line with the superordinate idea, to drive allometric FH-to-AGB models with RS data (like the FH product of the ESA BIOMASS mission),

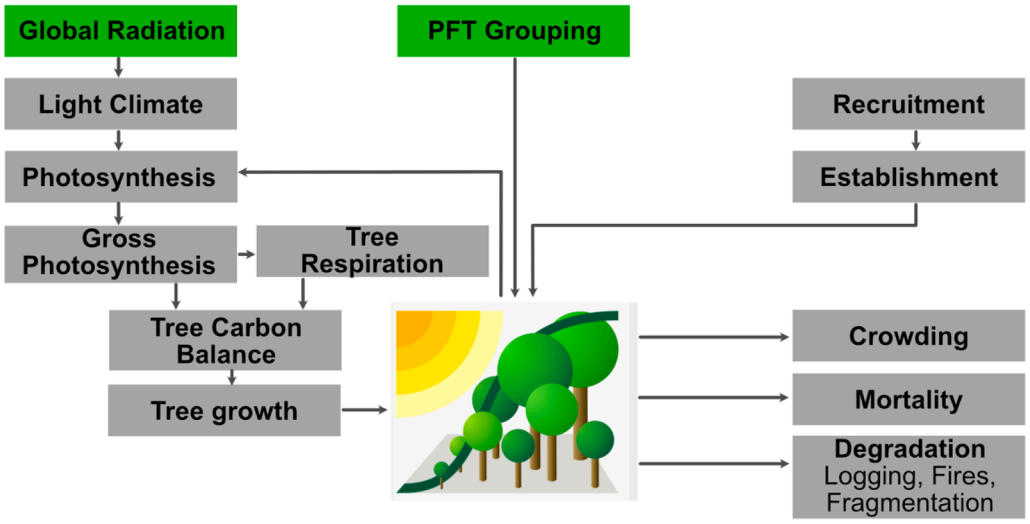

Fig. 1. Basic concept of the FORMIND forest gap model. The main processes are recruitment, establishment, mortality and growth. The model inputs (global radiation and PFT grouping) are marked in green. A full description of the model can be found on formind.org (adapted from Fischer et al., 2016; Rödig et al., 2017).

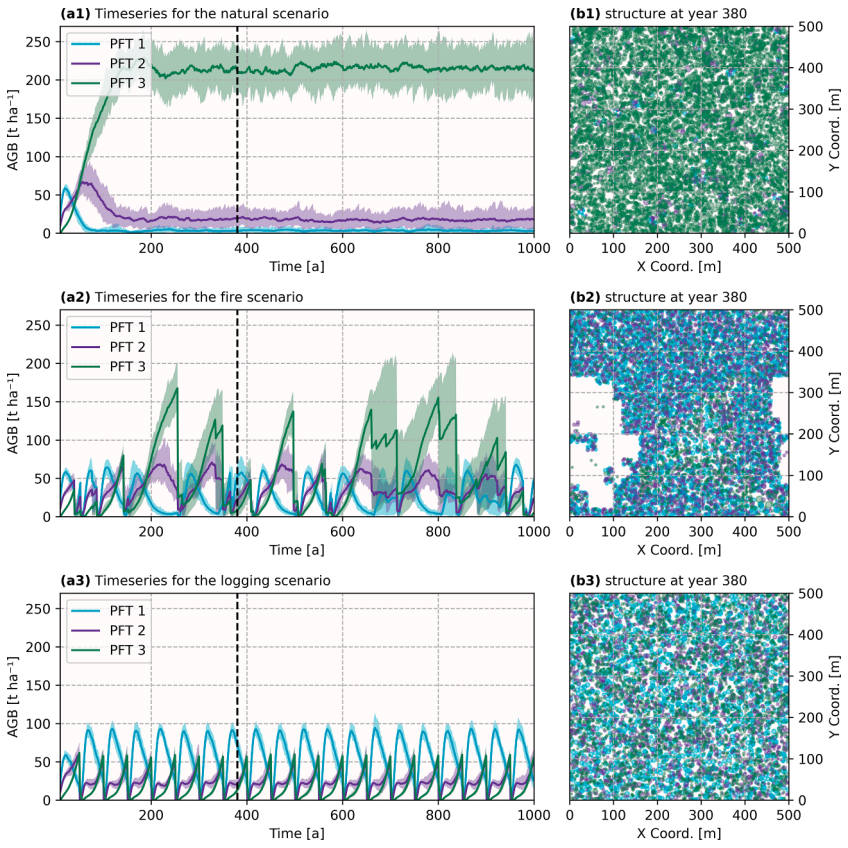

Fig. 2. (a1 to a3) Timeseries of the scenario simulation data for natural (a1), fire (a2) and logging scenarios (a3) (FORMIND forest model simulations of a 25 ha area). The colours indicate the different PFTs used in this analysis, with PFT 1 being a light demanding, fast growing species, PFT 2 an intermediate species and PFT 3 representing shade-tolerant late successional tree species. The shaded area around the timeseries shows the 90 % confidence band for results in ha patches. Figures in b1 to b3 show spatial simulation results of year 380 with dominating PFTs.

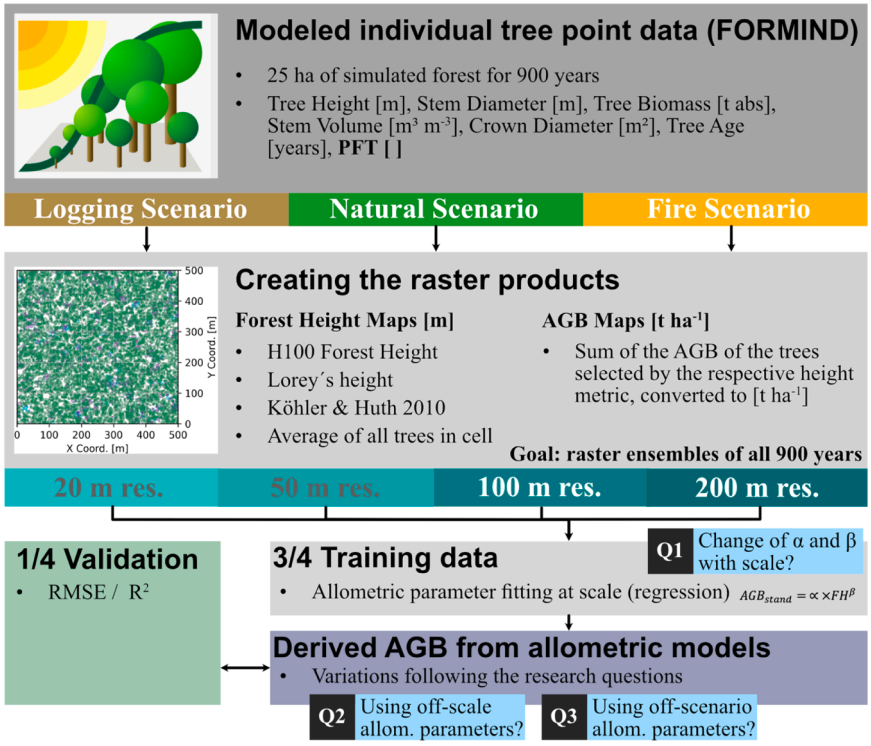

Fig. 3. Summary of the processing and analysis steps performed in this research.

we focus on FH specifications that resemble products generated by LiDAR and InSAR systems (see Fig. 3 for a schematic overview of our analysis).

In line with the BIOMASS FH product, the H100 standard forestry metric will be applied for the main analysis. The H100 rule has the advantage, that it roughly represents the forest height as seen by radar systems at different spatial scales (Hajnsek et al., 2009). The original H100 definition is defined as the average height of the 100 tallest trees within a 1 ha area (Philip, 1994). In the case presented in Eq. (5), the n-fraction of the 100 tallest trees will be used for sub-hectare analysis. The scale A in Eq. (6) defines the spatial resolution selected by the user and thus the number of trees included in the average. The number of trees is defined by n, each individual tree has the height H_i. Ultimately, the H100 height is calculated from the vector of the n-th highest H individual tree heights H_i. Resolutions finer than 20 m are excluded, as these would include few trees, or even singular trees in a 10 m × 10 m resolution case.

$$FH_{H100} = \frac{1}{n}\sum_{i=1}^{n} H_i \tag{5}$$

$$n = \left[100\ Trees \times \frac{A}{1\ ha}\right]\ for\ n > 1$$
$$H = \{H_1, H_2, \ldots, H_n,\}\ and\ H_1 \geq H_2 \geq \ldots \geq H_n \tag{6}$$

Also, the widely used Lorey's height (similar to a waveform LiDAR derived FH product) is added to the analysis. It is defined by the basal-area g weighted average individual tree heights within the selected spatial scale (Lorey, T., 1878):

$$FH_{Lorey} = \frac{\sum g \times H}{\sum g} \tag{7}$$

For intercomparison to the H100 and Lorey *FH* described in Eqs. (5), (6) and (7), the *FH* definition described in Köhler and Huth, 2010 is added (abbreviated as Köhler / Huth). This FH definition is applied at two resolution steps: 20 m × 20 m (0.04 ha) and 100 m × 100 m (1 ha). At 0.04 ha resolution, FH is defined as the height of the tallest tree within the 20 m × 20 m plot. At the 1 ha resolution, FH is calculated as the average of the tallest tree heights from each of the 25 individual 20 m × 20 m plots. The definition was accordingly extended to the 200 m × 200 m resolution, while the 50 m × 50 m resolution was omitted. Also, the arithmetic average value of all individual tree heights within the resolution cell is added.

These sampling methods can be segmented into two categories: a) the ones that only consider a quantile of the tree size distribution in the respective cell (H100 and Köhler / Huth), and b) the ones that observe and average the complete dataset and thus include the complete heterogeneity (Lorey, Averaging).

The AGB maps were produced in line with the FH definitions. For a) the biomass of the considered (thus the 'biggest') trees within the resolution cell was aggregated and converted to AGB densities. For b), the AGB of all trees was aggregated and converted. Thus, the case described in a represents the AGB of the plots canopy.

To mitigate the effects of the initial growth phase from bare soil, the first 100 years of the simulation data were clipped for the analysis. Naturally, regression-based scale analysis of the allometric parameters is not possible with a simulation covering just 25 ha, when the coarsest resolution is set to 4 ha. As the actual temporal succession of the forest is subordinate for this scale analysis, the individual years (25 ha) were rasterized and aggregated to a large raster ensemble, thus creating an area of 22,500 ha (15,000 m x 15,000 m). In this process, the rasterized cells of the individual years were kept together, as this spatial context is essential when observing the disturbance scenarios. Yet, to avoid spatial correlation in between the yearly cells, the raster batches of each year were randomly distributed on the resulting big raster.

2.4. Spatial scale analysis

The scale analysis was conducted at spatial resolutions of 20 m × 20 m, 50 m × 50 m, 100 m × 100 m and 200 m × 200 m. For briefness, we will refer to these as 20 m, 50 m, 100 m, and 200 m. For the statistical analysis, the resulting raster ensembles were divided into a training set (3/4) and a validation set (1/4). To investigate the effect of a changing spatial scale on the allometric parameters, these parameters were fitted to the corresponding FH and AGB datasets at each resolution using non-linear least squares fitting. Each regression analysis was carried out with a sampling size of 3500 raster cells to ensure that the process would not be biased through an uneven amount of data points between the resolution steps. The regression analysis was repeated 500 times to grasp the spatial variability. The resulting parameter values are the average of these repetitions. Boundaries are defined for α [$\alpha > 0$] and β [$0 < \beta < 3$], for both to remain in ranges similar to results in literature (Köhler and Huth, 2010). With this, baseline results are obtained at the 'correct' and interrelated resolutions steps. This represents the optimal case, as it makes use of the highest possible data density and strong aggregation across the created raster ensemble. Since such conditions are not available in practice, the baseline quantifies the error introduced solely by the regression and the model's inherent capabilities. We can then compare this baseline to more realistic, restricted models.

To assess the effect of using off-scale allometric parameters (see Q2), two cases (C1 and C2) were defined. In C1, the 20 m parameters from the baseline results are applied to the coarser resolution scales FH maps and subsequently compared to the respective baseline validation AGB datasets. For C2, only the β exponent is obtained from the 20 m results and kept constant over scales. The allometric factor α is fitted to the 'correct' resolution scale. In line with attributing a physical significance to the allometric parameters, we decided against a local adaption of β, as it is attributed to the forest type, which by itself is expected to be less variable with scale. An analysis based on global vegetation structure data carried out by Ni-Meister et al., 2022 showed that β is largely constant across global forest biomes except boreal forest. The resulting modelled AGB values are again compared to the corresponding validation AGB sets.

Lastly for the third research aim, parameter sets from different simulation scenarios were interchanged. For our case, the parameter sets obtained from heavily degraded forests (fire and logging) are applied to the FH dataset of the natural scenario, to form derived off-scenario AGB datasets. Those are then again compared to the on-scenario validation results of the individual scale.

The entire processing scheme is visualized in the flowchart of Fig. 3.

3. Results

3.1. General results from the rasterization of the forest model data

Irrespective of the sampling method, the variance of FH and AGB values was high at the 20 m scale (Fig. 4). At a resolution of 20 m, the AGB changed between 20 t ha^{-1} and almost 500 t ha^{-1} for the H100 and Lorey sampling methods. For Figs. 4 and 5, we will focus on these two sampling methods as they represent the most realistic cases and feature the mentioned direct relationship to RS derived FH products. Whilst the FH range is equal for both sampling methods, Lorey sampling shows slightly higher AGB values compared to H100 (maximum at 479 t ha^{-1}). For a simplified visualization, the distributions are added in the form of kernel density estimations (KDE). Both the FH and AGB distributions collapse with higher scales, yet a higher AGB variance is visible across scales if compared to the FH frequencies. Average values for FH and AGB (H100 / Lorey) settle at 23 / 26 m and 193 / 236 t ha^{-1} respectively. A slight right shift of the FH and AGB frequencies (see the KDE subplots b1, c1 of Fig. 4) is observable in the H100 results, thus prioritizing taller trees at larger scales. By contrast to the Lorey sampling results, the distributions of the H100 sampling collapse disproportional with scale,

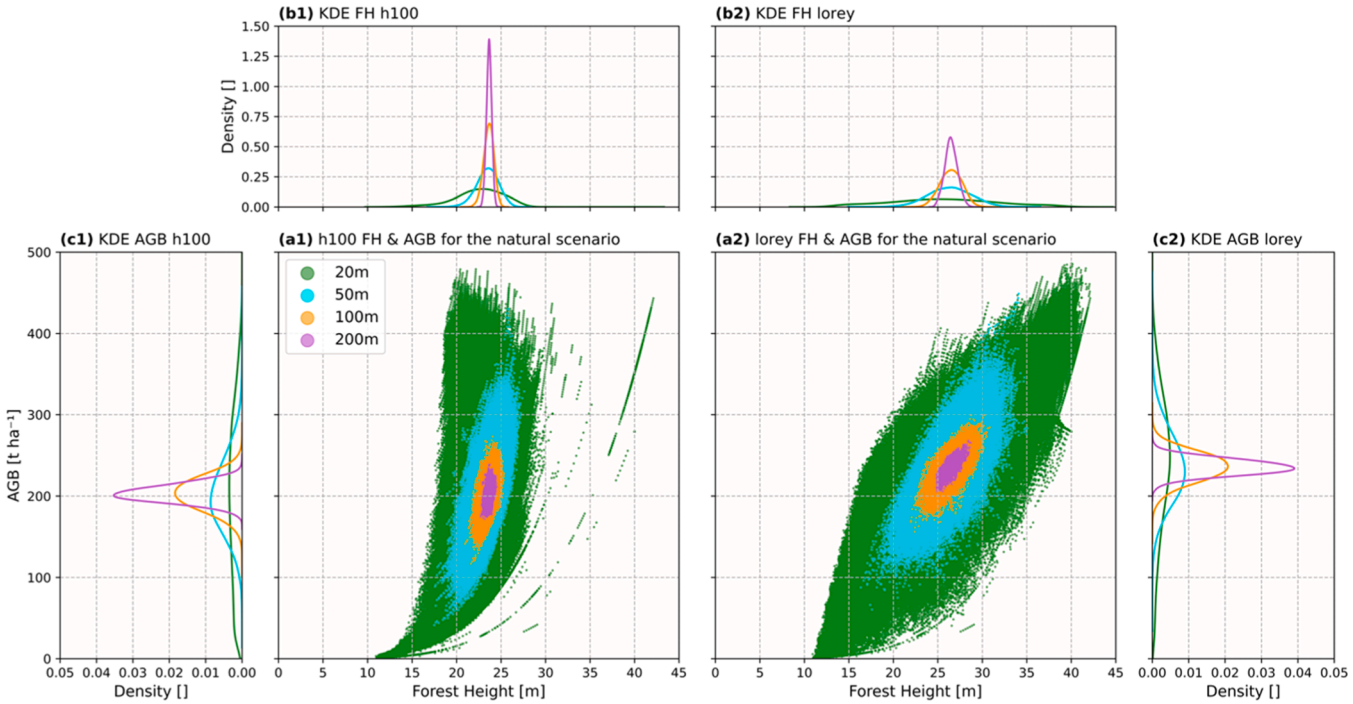

Fig. 4. FH and AGB point clouds at the different resolution scales (colours) with corresponding frequency distributions abstracted by a Kernel Density Estimation (KDE) function for the natural scenario. The individual trees were rasterized according to the H100 (a1, b1, c1) and Lorey (a2, b2, c2) FH sampling methods. Note that the linear features are caused by raster cells in the ensemble, where the stand density is very low, or even composed of a singular tree after the respective sampling method. Thus, no stand heterogeneity exists resulting in theses near 'optimal' allometric curves.

thus forming a near vertical FH to AGB point cloud at the BIOMASS mission scale of 200 m. Lorey sampling meanwhile maintains higher variances across scales.

In contrast to the natural scenario, the disturbance scenarios show considerably less homogenous FH and AGB distributions for all scales, given the much higher variability in species / PFT composition at any year of the simulation (Fig. 5). Also, an increased variance across both simulation scenarios is visible compared to the natural simulation. Anomalous horizontal patterns are visible for AGB values around 100 t ha^{-1} in the logging scenario. Whereas for the H100 sampling, a slight positive correlation between FH and AGB is observable, while the opposite occurs for Lorey.

3.2. Change of the allometric parameters α and β with scale

Considerable changes, but no trends in the parameters α and β of the allometric function could be observed over scales, simulation scenarios and sampling methods (Fig. 6). The step from 20 m to 50 m scales consistently showed the biggest fluctuations. For α, the logging scenario shows the lowest values of all three forest states and sampling methods. The saturation of β near the value 3 is caused by its upper bound definition. For the natural scenario, β values decrease from 50 m upwards and increase for the disturbance scenarios. An opposed development for α and β over the scales is noticeable for the non-extreme values. The RMSE decreases with scale for all scenarios and sampling methods. On average, the smallest residual errors were observed for the logging scenario. Regarding the R^2 coefficient, again no clear statement on the development with scales, or the comparison between scenarios can be given. Köhler/Huth sampling returns the highest values, while the average sampling performs worst. Focusing on the comparison of H100 and Lorey sampling, the latter performs slightly better for the natural scenario, whereas H100 outperforms Lorey for the degraded forest simulations.

3.3. Transferability of allometric parameters between spatial resolutions

Fig. 7 summarizes the transferability of the allometric parameters across the spatial resolutions. If α and β are kept constant, RMSE values increased for the natural and fire scenario compared to the baseline scenario. This relative RMSE increase becomes more prominent for higher resolution scales. Irrespective of the sampling method, RMSE values did not change by using off-scale parameters for the logging scenario. If only β is kept constant, both R^2 and RMSE values were close to the baseline values in the natural and disturbance scenarios. Interestingly, R^2 values of constant α and β parameters were higher than compared to the baseline scenario, or for results with a constant value for α. Overall, H100 sampling performs better for the fire and logging scenario, while Lorey sampling delivers more robust relationships in the natural scenario.

3.4. Results on using off-scenario allometric parameters (Q3)

If allometric functions of the natural scenario had been applied to fire and logging scenarios, AGB would have been generally underestimated (Fig. 8). This effect was even stronger for the logging scenario compared to the fire scenario and if spatial scales increased to 100 m and 200 m. No change in the distribution between validation AGB to derived AGB have been observed, indicating a linear shift of the AGB point clouds.

4. Discussion

Overall, the range of the FH and AGB (as well as their relationship) is comparable to results from studies in tropical forest ecosystems (Armstrong et al., 2020; Köhler and Huth, 2010; Rödig et al., 2017; Saatchi et al., 2011). However, variances in the relationship between AGB and FH were higher compared to previous studies, which is explained in the following. The high AGB variance is caused by the combination of the different weighting of the individual height to AGB allometries, the changes of stand density and both the FH sampling and

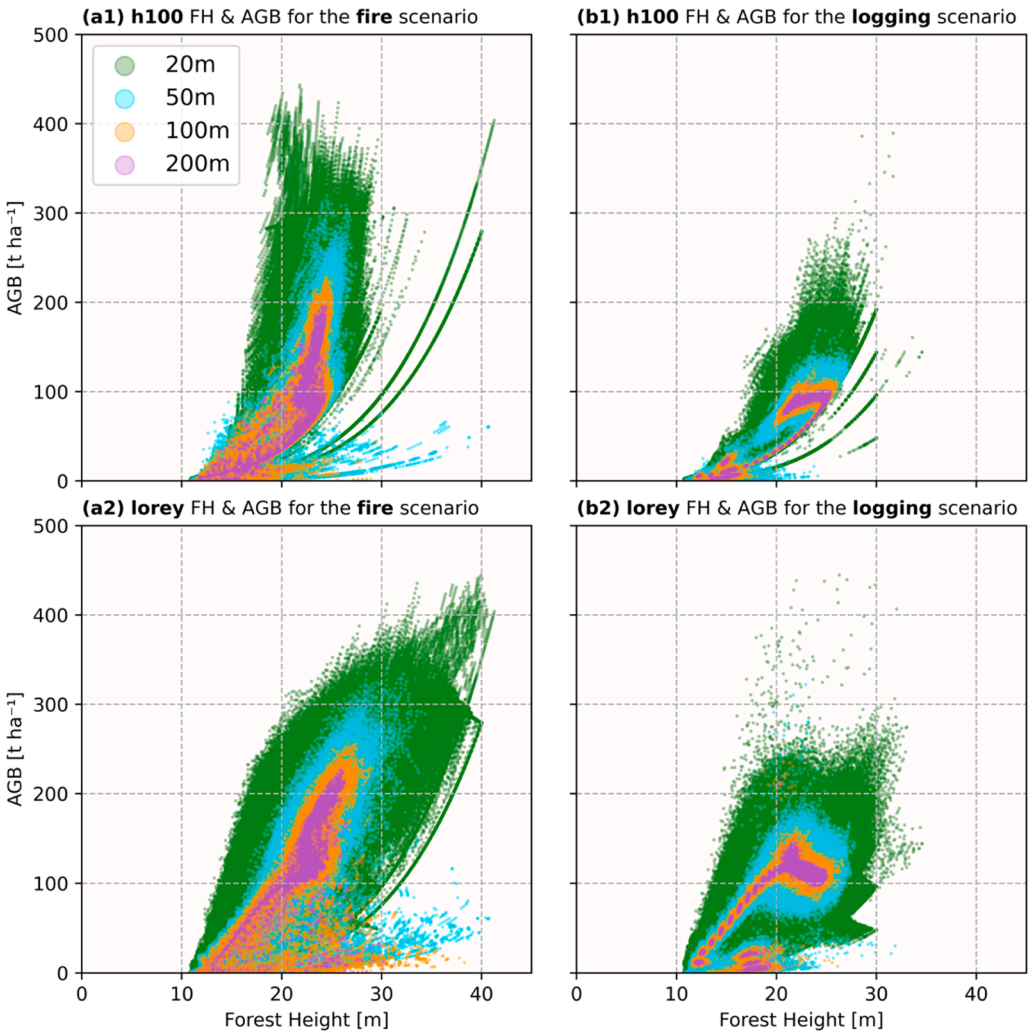

Fig. 5. FH and AGB distributions for the fire (left column) and logging (right column) scenarios. Upper and lower rows show results for H100 and Lorey sampling methods, respectively. Colours indicate different spatial scales.

temporal succession of the forest patches in the raster ensemble. This also explains the highly asymmetric relationship between the FH and AGB KDE distributions. Forest patches can have the same FH but considerably differ in stand densities. In addition, following the temporal aggregation of the individual simulation years, the relationship between growth of the trees and increase in DBH (so AGB assimilation) is not linear (Pan et al., 2013). The increased AGB density values for the Lorey sampling are caused by the rasterization and sampling method. In contrast to H100, all trees were assessed for the AGB density. By weighing the contribution of the singular trees by their respective basal area, very similar ranges of FH are achieved as with H100 sampling, because mature trees are given a higher relevance. Yet, the AGB of the Lorey sampling is higher than the H100 AGB. In line with expectations and the simulation inputs, a considerable decrease of AGB values is caused by disturbance of the forest. For the fire and logging scenario, the high wood density and slow growing PFT3 has little chance to establish – thus the AGB development potential of these forest patches is widely deteriorated. For coarser spatial scales, the ranges of FH and AGB decreased, which is in line with results from Huth, Drechsler and Köhler, 2005; Armstrong et al., 2020. In the FH-to-AGB correlation of the disturbance scenarios, the horizontal features or even the partly negative correlations are caused by the high PFT mixing at intermediate FH values resulting in trees with similar FH, but considerably different AGB, due to differences in the specific wood density.

4.1. *Change of the allometric parameters with scale*

In general, no clear trend is visible for both α and β, but considerable fluctuations in both parameters are visible across spatial scales, sampling methods and disturbance scenarios. Again, considering the different scope of the presented sampling methods, a comparability between the allometric parameters resulting the regression analysis of the different FH and AGB maps is not expected, as every sampling method 'sees' a slightly different forest canopy composition. Similar results are visible in Köhler and Huth, 2010. The lowest values for α occur for the logging scenario across all sampling methods, which can be explained by the considerably smaller stand density (Köhler and Huth, 2010).

The decrease of R^2 with scale that is evident in Armstrong et al., 2020 cannot be completely reproduced in our work. While Köhler and Huth, 2010 also show a slight decrease in R^2 from 61.4 % (20 m scale) to 58.1 % (100 m) with their sampling method, our results did not show a uniform decrease across all sampling methods. Especially the highly disturbed forest scenarios showed consistent or even improving R^2 coefficients, which is caused by the decreased variability in FH and AGB that thus improves the model precision in these scenarios. The advantage of Lorey sampling over H100 in the natural scenario is evident from the point cloud, as Lorey sampling produces less steep datasets by regaining a higher FH variability also in higher scales.

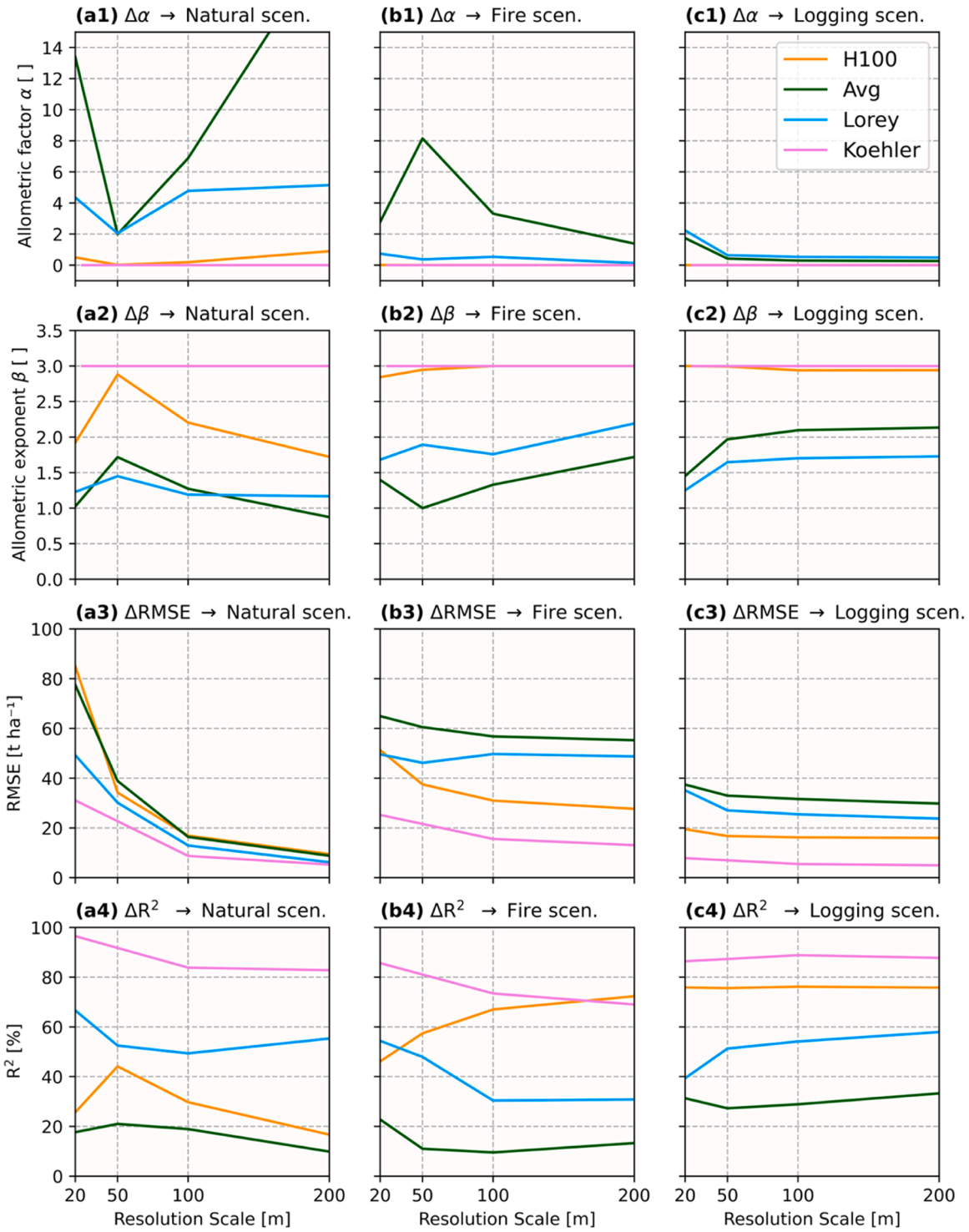

Fig. 6. Change of the allometric parameters α (first row) and β (second), the RMSE (third) and R^2 (fourth) with scale, FH sampling method (colours) and simulation scenario natural (first column), fire (second) and logging (third). Overall, the Koehler / Huth sampling performs best. Contrary to that, the average sampling yields the worst results. Concerning Lorey sampling and H100, Lorey performs better for the natural scenario, whereas H100 has an advantage in the fire and logging simulations.

4.2. Effect of using off-scale allometries

Two different concepts have been applied to test if allometric functions derived at 20 m can be applied to coarser resolution data. In the first case, α and β were fixed to the 20 m baseline values, which resulted in an additional error that increases for coarser scales at the fire and natural scenarios. In contrast, no changes in RMSE are observed for the logging scenario. As the logging scenario has relatively constant values for the allometric parameters across the resolution scales (see Fig. 6), no prominent change emerges in this case. In the second case, only β is constant to simulate a localized function that estimates the local stand density. Overall, this showed a near perfect mitigation of the additional errors emerging from C1.

Consequently, for the natural scenario considerable errors arise from

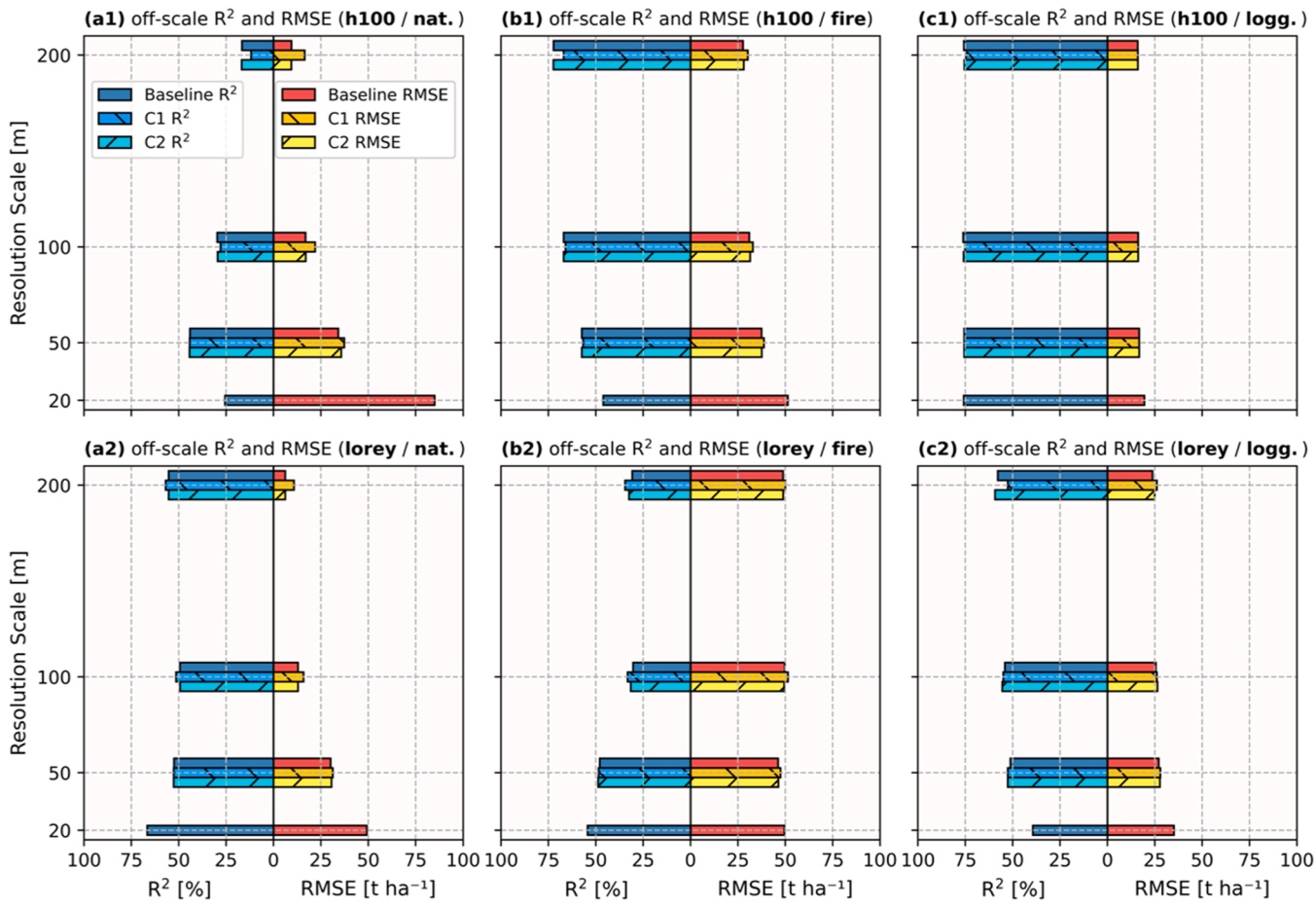

Fig. 7. Summary of the R^2 and RMSE results for the baseline (Q1), the case where α and β have been kept constant (C1) and the case where only α has been kept constant (C2). Upper and lower rows show results for H100 and Lorey sampling methods, respectively. Columns represent the natural, fire and logging scenarios.

using off-scale allometric parameters for natural forests. Therefore, a RS driven function that creates localized estimates for the forest structure might reduce these errors. For the fire scenario, the effect is less prominent and for logging regimes, no relevant dependency of the allometric parameters and thus the quality of the simulation is observable with scale. The question needs to be addressed, at which accuracy α must be estimated. Given that our approach offers a hypothetical albeit unrealistic optimum, we suggest that a coarser classification of α will be sufficient and feasible.

4.3. Effect of forest disturbance on AGB allometries

In general, and in line with expectations, a strong underestimation of the AGB occurs if allometries trained for degraded forests (in this case from the forest and logging scenarios) are applied to FH maps of old-growth forest patches. The cause for this is that in our results we are applying parameter sets that were specifically optimized for degraded forests to FH maps (and AGB ensembles) of old-growth forest patches, which features the highest possible AGB densities for our model initialization. This additional error is substantial and becomes even more prominent with coarsening scales. The consequence is that especially at coarser scales, the knowledge on the successional state of the forest or degradation status is important. Since derivation of such data in potentially highly fragmented and heterogenous areas is challenging especially at coarse spatial resolutions, this must be analysed in future research.

4.4. Implications for future research

Given the indisputable role of tree height (or FH at the non-individual scale) as predictor for AGB and the upcoming FH and structure products of the ESA BIOMASS mission, the usage of the described FH-to-AGB allometries will play a key role for large-scale AGB estimations (Armstrong et al., 2020; Quegan et al., 2019; Saatchi et al., 2011). Yet, their inherent limitations of transferability and scalability remain. To address these limitations, the allometric function can be expanded by attributing the α and β parameters to semi-physical properties and regionalize those with high resolution RS datasets. This, however, poses additional challenges concerning the scalability and comparability of the applied RS and FI datasets. This paper addressed the application of directly using allometric parameters to much coarser resolution FH maps, as well as strategies to mitigate the introduced uncertainty.

For this, the IBGM FORMIND offers a unique opportunity, as it forms the perfect basis to directly investigate forest structure at multiple scales at the commodity and cost effectiveness of modelled datasets (Armstrong et al., 2020). PFTs offer a simplified approach to facilitate model parametrization in extremely diverse ecosystem such as the Amazonas lowland rainforest considered in this work. Still, dynamic and functional plant trait diversity is heavily neglected by the PFT approach. Just as in the parametrization of this work, mean values from FI datasets are used to describe photosynthetic capacity, wood density and leaf turnover times a priori. Even though FORMIND incorporates these key inputs to simulate tree growth, mortality, competition and recruitment at gap level, plant strategies are set into limited boundaries. Especially under global change scenarios, PFTs do not have the capability to sufficiently follow alternating plant trait combinations, often leading to

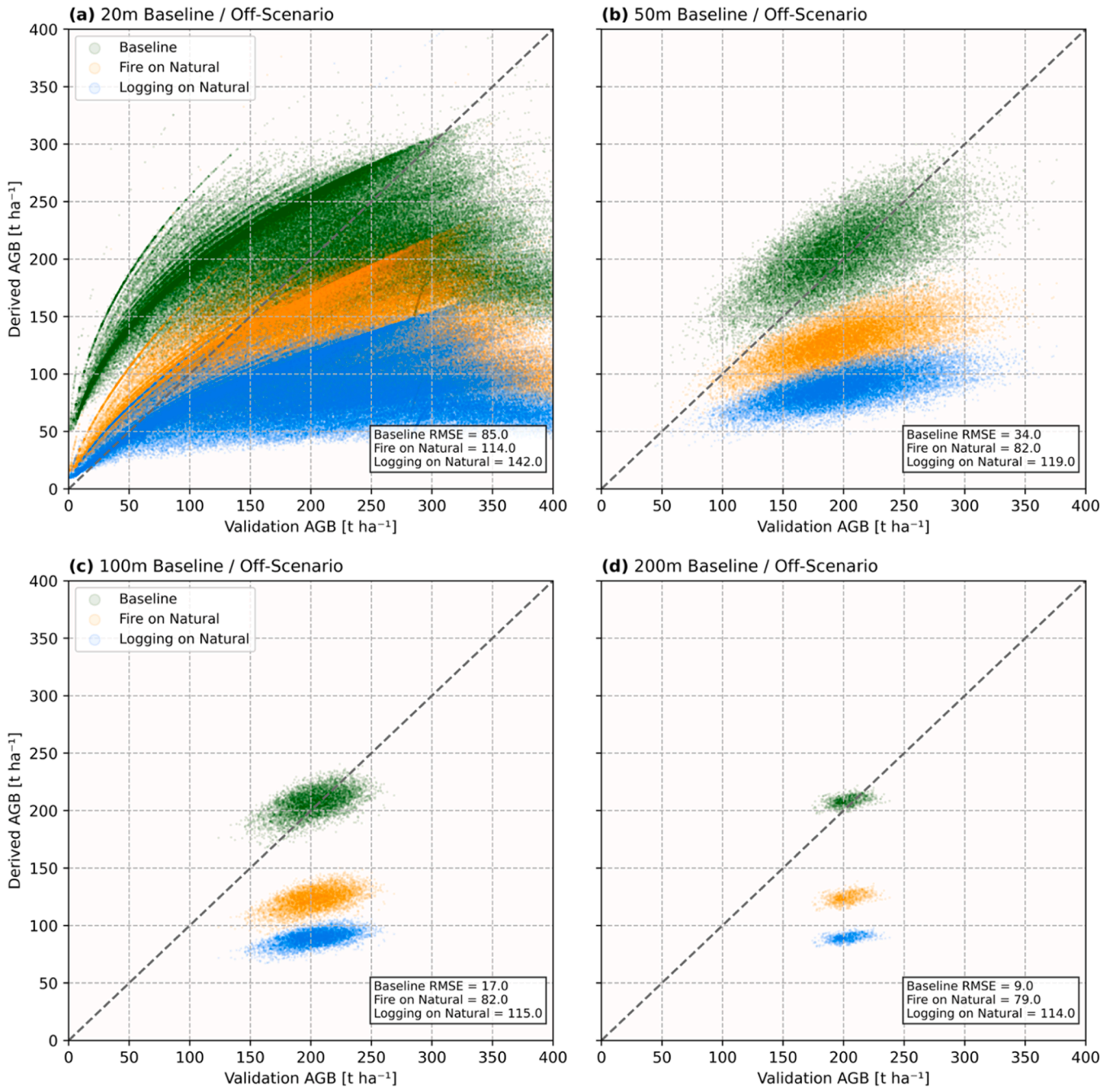

Fig. 8. Off-scenario analysis for the natural scenario (baseline) under H100 sampling for 20 m (a), 50 m (b), 100 m (c) and 200 m spatial scales (d). Simulation scenarios are indicated by colour.

overreaction in predicting ecosystem response. New, trait-based vegetation models with functional trade-offs are needed to increase modelling accuracy of carbon cycle processes (Fyllas et al., 2014; Pavlick et al., 2013; Rius et al., 2023). This heavily increased complexity comes with the major drawbacks of a highly complex initialization and significantly increased modelling times. For our application, a trait-based approach is not required. Even though we model 1000 years of forest succession in all three scenarios, environmental changes are not considered, and a dynamic adaption of plant traits and interconnections is secondary. FORMIND as a model and the model parametrization used in this study was proven successful in depicting ABG dynamics across forest succession and disturbance dynamics (Fischer et al., 2016; Rödig et al., 2018 2017). Also, a study by Fischer et al., 2018 demonstrated that three PFTs are sufficient to realistically grasp forest succession and simulate disturbances.

By incorporating realistic forest degradation scenarios, a shift towards a much broader perspective in forest structure analysis becomes viable. In contrast, FI datasets are often either located in prime old-growth locations, or in highly degraded forests. Thus both the representativeness and transferability is impeded when using those in combination with RS products (Fischer et al., 2016; Köhler and Huth, 2010). The main downside of applying an IBGM in our analysis lies in the lack of the representation of natural heterogeneity due to the abstraction inherent to models. With the simulation environment produced by FORMIND and the near optimal process of the least-squares regression (within its obvious limitations), the resulting absolute errors and margins are likely considerably smaller compared to real world datasets and scenarios.

This study does not intend to find the 'best' sampling method to create a FH map from individual tree datapoints. The four methods H100, Lorey, Averaging and Köhler/Huth were included to improve the comparability to existing work, as well to provide a wider range of commonly used definitions in forest ecology (Armstrong et al., 2020). Moreover, it is important to both highlight the implications and limitations of the different sampling methods and create awareness for resulting FH and AGB changes in dynamic scenarios. Two main concerns arise: first, the FH distribution (and so the AGB) shifts to higher values for segmenting sampling methods, as only the n^{th} highest trees are considered to form the FH and AGB raster datasets. Thus, a segmentation and partially very drastic restriction of the natural heterogeneity occurs, while coarser resolutions render higher values for FH and AGB. For the non-segmenting, averaging sampling methods with all trees being considered, a generally higher AGB density is achieved. In both cases, the question could be asked, which method is better suited for applications to satellite data. In practise, these considerations must also encompass data availability and/or cost effectiveness if additional datasets must be developed. Given such future datasets (like the ESA BIOMASS FH product), work needs to be done to close the gap between creating a uniform definition for the FH from RS and then the bottom-up sampling of the individual trees from either FI or simulation for the regression analysis of the allometric parameters.

5. Conclusion

In summary, our study emphasizes the importance of interpreting the driving factors and dependencies of FH-to-AGB allometric functions. In light of the ever-growing availability of RS data, multi-sensoral, multi-scale and multi-temporal analyses will become more feasible. Especially for AGB estimation, FH driven allometries will play a major role, also with the upcoming BIOMASS mission and existing and on-going GEDI or TerraSAR-X / TanDEM-X missions. However, a consideration of local forest structure at a higher spatial resolution is key to reduce uncertainties and to improve model precision. Scale analysis to assess comparability and compatibility of different datasets is essential, but seldom implemented. With our study, we showed with a regression-based approach and using FORMIND model data that allometric factors vary with scale, and that these fluctuations are highly dependent on the FH sampling method and forest disturbance scenario. Using allometric parameters from 'wrong' spatial scales is possible but adds a significant error to the AGB estimate. To mitigate this error, we simulated a potential forest structure function that could be driven by higher resolution remote sensing data to mitigate the additional error. Given this, we also emphasize the importance of knowing the forest condition *a priori*. Both for stand density estimates, but especially for forest disturbance with vastly different AGB potentials, precise and high-resolution structure references are needed.

Funding

This work was conducted with funding from the German Space Agency (DLR-RFM) and the Federal Ministry for Economic Affairs and Climate Action (BMWI) under the grant number 50EE2111.

CRediT authorship contribution statement

Benedikt Hartweg: Writing – original draft, Visualization, Validation, Software, Resources, Project administration, Methodology, Investigation, Formal analysis, Data curation, Conceptualization. **Leonard Schulz:** Resources. **Andreas Huth:** Writing – review & editing, Methodology, Conceptualization. **Konstantinos Papathanassiou:** Writing – review & editing, Supervision, Conceptualization. **Lukas W. Lehnert:** Writing – review & editing, Supervision, Resources, Project administration, Conceptualization.

Declaration of competing interest

The authors declare that they have no known competing financial interests or personal relationships that could have appeared to influence the work reported in this paper.

Data availability

Data will be made available on request.

References

Armstrong, A.H., Huth, A., Osmanoglu, B., Sun, G., Ranson, K.J., Fischer, R., 2020. A multi-scaled analysis of forest structure using individual-based modeling in a costa rican rainforest. Ecol. Modell. 433, 109226. https://doi.org/10.1016/j.ecolmodel.2020.109226.

Brondizio, E.S., Batistella, M., Moran, E.F., 2009. LBA-ECO LC-09 vegetation composition and structure in the Brazilian Amazon: 1992-1995 2.516334 MB. https://doi.org/10.3334/ORNLDAAC/939.

Chave, J., Andalo, C., Brown, S., Cairns, M.A., Chambers, J.Q., Eamus, D., Fölster, H., Fromard, F., Higuchi, N., Kira, T., Lescure, J.-P., Nelson, B.W., Ogawa, H., Puig, H., Riéra, B., Yamakura, T., 2005. Tree allometry and improved estimation of carbon stocks and balance in tropical forests. Oecologia 145, 87–99. https://doi.org/10.1007/s00442-005-0100-x.

Chave, J., Davies, S.J., Phillips, O.L., Lewis, S.L., Sist, P., Schepaschenko, D., Armston, J., Baker, T.R., Coomes, D., Disney, M., Duncanson, L., Hérault, B., Labrière, N., Meyer, V., Réjou-Méchain, M., Scipal, K., Saatchi, S., 2019. Ground data are essential for biomass remote sensing missions. Surv. Geophys. 40, 863–880. https://doi.org/10.1007/s10712-019-09528-w.

Chave, J., Muller-Landau, H.C., Baker, T.R., Easdale, T.A., Steege, H.T., Webb, C.O., 2006. Regional and phylogenetic variation of wood density across 2456 neotropical tree species. Ecol. Appl. 16, 2356–2367. https://doi.org/10.1890/1051-0761(2006)016[2356:RAPVOW]2.0.CO;2.

Chave, J., Réjou-Méchain, M., Búrquez, A., Chidumayo, E., Colgan, M.S., Delitti, W.B.C., Duque, A., Eid, T., Fearnside, P.M., Goodman, R.C., Henry, M., Martínez-Yrízar, A., Mugasha, W.A., Muller-Landau, H.C., Mencuccini, M., Nelson, B.W., Ngomanda, A., Nogueira, E.M., Ortiz-Malavassi, E., Pélissier, R., Ploton, P., Ryan, C.M., Saldarriaga, J.G., Vieilledent, G., 2014. Improved allometric models to estimate the aboveground biomass of tropical trees. Glob. Chang. Biol. 20, 3177–3190. https://doi.org/10.1111/gcb.12629.

Choi, C., Pardini, M., Heym, M., Papathanassiou, K.P., 2021. Improving forest height-to-biomass allometry with structure information: a tandem-X study. IEEE J. Sel. Top. Appl. Earth Observat. Remote Sens. 14, 10415–10427. https://doi.org/10.1109/JSTARS.2021.3116443.

Erb, K.-H., Kastner, T., Plutzar, C., Bais, A.L.S., Carvalhais, N., Fetzel, T., Gingrich, S., Haberl, H., Lauk, C., Niedertscheider, M., Pongratz, J., Thurner, M., Luyssaert, S., 2018. Unexpectedly large impact of forest management and grazing on global vegetation biomass. Nature 553, 73–76. https://doi.org/10.1038/nature25138.

Fischer, R., 2021. The long-term consequences of forest fires on the carbon fluxes of a tropical forest in Africa. Appl. Sci. 11, 4696. https://doi.org/10.3390/app11104696.

Fischer, R., Bohn, F., Dantas de Paula, M., Dislich, C., Groeneveld, J., Gutiérrez, A.G., Kazmierczak, M., Knapp, N., Lehmann, S., Paulick, S., Pütz, S., Rödig, E., Taubert, F., Köhler, P., Huth, A., 2016. Lessons learned from applying a forest gap model to understand ecosystem and carbon dynamics of complex tropical forests. Ecol. Modell. 326, 124–133. https://doi.org/10.1016/j.ecolmodel.2015.11.018.

Fischer, R., Rödig, E., Huth, A., 2018. Consequences of a reduced number of plant functional types for the simulation of forest productivity. Forests. 9, 460. https://doi.org/10.3390/f9080460.

Fyllas, N.M., Gloor, E., Mercado, L.M., Sitch, S., Quesada, C.A., Domingues, T.F., Galbraith, D.R., Torre-Lezama, A., Vilanova, E., Ramírez-Angulo, H., Higuchi, N., Neill, D.A., Silveira, M., Ferreira, L., Aymard, C., G, A., Malhi, Y., Phillips, O.L., Lloyd, J., 2014. Analysing Amazonian forest productivity using a new individual and trait-based model (TFS v.1). Geosci. Model. Dev. 7, 1251–1269. https://doi.org/10.5194/gmd-7-1251-2014.

Hajnsek, I., Kugler, F., Lee, S.-K., Papathanassiou, K.P., 2009. Tropical-forest-parameter estimation by means of Pol-InSAR: the INDREX-II campaign. IEEE Trans. Geosci. Remote Sens. 47, 481–493. https://doi.org/10.1109/tgrs.2008.2009437.

Hetzer, J., Huth, A., Wiegand, T., Dobner, H.J., Fischer, R., 2020. An analysis of forest biomass sampling strategies across scales. Biogeosciences. 17, 1673–1683. https://doi.org/10.5194/bg-17-1673-2020.

Huth, A., Drechsler, M., Köhler, P., 2005. Using multicriteria decision analysis and a forest growth model to assess impacts of tree harvesting in Dipterocarp lowland rain forests. For. Ecol. Manage 207, 215–232. https://doi.org/10.1016/j.foreco.2004.10.028.

Kazmierczak, M., Wiegand, T., Huth, A., 2014. A neutral vs. non-neutral parametrizations of a physiological forest gap model. Ecol. Modell. 288, 94–102. https://doi.org/10.1016/j.ecolmodel.2014.05.002.

Köhler, P., Huth, A., 2010. Towards ground-truthing of spaceborne estimates of above-ground life biomass and leaf area index in tropical rain forests. Biogeosciences. 7, 2531–2543. https://doi.org/10.5194/bg-7-2531-2010.

Kunert, N., Aparecido, L.M.T., Higuchi, N., Santos, J.D., Trumbore, S., 2015. Higher tree transpiration due to road-associated edge effects in a tropical moist lowland forest.

Agric. For. Meteorol. 213, 183–192. https://doi.org/10.1016/j.agrformet.2015.06.009.
Le Toan, T., Quegan, S., Davidson, M.W.J., Balzter, H., Paillou, P., Papathanassiou, K., Plummer, S., Rocca, F., Saatchi, S., Shugart, H., Ulander, L., 2011. The BIOMASS mission: mapping global forest biomass to better understand the terrestrial carbon cycle. Remote Sens. Environ. 115, 2850–2860. https://doi.org/10.1016/j.rse.2011.03.020.
Lewis, S.L., Edwards, D.P., Galbraith, D., 2015. Increasing human dominance of tropical forests. Science (1979) 349, 827–832. https://doi.org/10.1126/science.aaa9932.
Lorey, T., 1878. Die mittlere Bestandshöhe (transl: 'The mean stock height'). Allgemeine Forst-und Jagdzeitung 54, 149–155.
Mette, K.P.T., 2004. Applying a common allometric equation to convert forest height from Pol-InSAR data to forest biomass. In: IEEE International IEEE International IEEE International Geoscience and Remote Sensing Symposium, 2004. IGARSS '04, 2004. IEEE. https://doi.org/10.1109/igarss.2004.1369013. Proceedings.
Meyer, V., Saatchi, S.S., Chave, J., Dalling, J.W., Bohlman, S., Fricker, G.A., Robinson, C., Neumann, M., Hubbell, S., 2013. Detecting tropical forest biomass dynamics from repeated airborne lidar measurements. Biogeosciences. 10, 5421–5438. https://doi.org/10.5194/bg-10-5421-2013.
Mo, L., Zohner, C.M., Reich, P.B., Liang, J., De Miguel, S., Nabuurs, G.-J., Renner, S.S., van den Hoogen, J., Araza, A., Herold, M., 2023. Integrated global assessment of the natural forest carbon potential. Nature 624, 92–101.
Neuville, R., Bates, J.S., Jonard, F., 2021. Estimating forest structure from UAV-mounted LiDAR point cloud using machine learning. Remote Sens. (Basel) 13, 352. https://doi.org/10.3390/rs13030352.
Ni-Meister, W., Rojas, A., Lee, S., 2022. Direct use of large-footprint lidar waveforms to estimate aboveground biomass. Remote Sens. Environ. 280, 113147. https://doi.org/10.1016/j.rse.2022.113147.
Pan, Y., Birdsey, R.A., Phillips, O.L., Jackson, R.B., 2013. The structure, distribution, and biomass of the world's forests. Annu Rev. Ecol. Evol. Syst. 44, 593–622. https://doi.org/10.1146/annurev-ecolsys-110512-135914.
Pavlick, R., Drewry, D.T., Bohn, K., Reu, B., Kleidon, A., 2013. The Jena Diversity-Dynamic Global Vegetation Model (JeDi-DGVM): a diverse approach to representing terrestrial biogeography and biogeochemistry based on plant functional trade-offs. Biogeosciences. 10, 4137–4177. https://doi.org/10.5194/bg-10-4137-2013.
Philip, M.S., 1994. Measuring Trees and Forests, 2. ed., repr. ed. CABI Publishing, Wallingford.
Pilli, R., Anfodillo, T., Carrer, M., 2006. Towards a functional and simplified allometry for estimating forest biomass. For. Ecol. Manage 237, 583–593. https://doi.org/10.1016/j.foreco.2006.10.004.
Quegan, S., Le Toan, T., Chave, J., Dall, J., Exbrayat, J.-F., Minh, D.H.T., Lomas, M., D'Alessandro, M.M., Paillou, P., Papathanassiou, K., Rocca, F., Saatchi, S., Scipal, K., Shugart, H., Smallman, T.L., Soja, M.J., Tebaldini, S., Ulander, L., Villard, L., Williams, M., 2019. The European Space Agency BIOMASS mission: measuring forest above-ground biomass from space. Remote Sens. Environ. 227, 44–60. https://doi.org/10.1016/j.rse.2019.03.032.
Rius, B.F., Filho, J.P.D., Fleischer, K., Hofhansl, F., Blanco, C.C., Rammig, A., Domingues, T.F., Lapola, D.M., 2023. Higher functional diversity improves modeling of Amazon forest carbon storage. Ecol. Modell. 481, 110323. https://doi.org/10.1016/j.ecolmodel.2023.110323.
Rödig, E., Cuntz, M., Heinke, J., Rammig, A., Huth, A., 2017. Spatial heterogeneity of biomass and forest structure of the Amazon rain forest: linking remote sensing, forest modelling and field inventory. Global Ecol. Biogeogr. 26, 1292–1302. https://doi.org/10.1111/geb.12639.
Rödig, E., Cuntz, M., Rammig, A., Fischer, R., Taubert, F., Huth, A., 2018. The importance of forest structure for carbon fluxes of the Amazon rainforest. Environ. Res. Lett. 13, 054013. https://doi.org/10.1088/1748-9326/aabc61.
Saatchi, S.S., Harris, N.L., Brown, S., Lefsky, M., Mitchard, E.T.A., Salas, W., Zutta, B.R., Buermann, W., Lewis, S.L., Hagen, S., Petrova, S., White, L., Silman, M., Morel, A., 2011. Benchmark map of forest carbon stocks in tropical regions across three continents. Proceed. National Acad. Sci. 108, 9899–9904. https://doi.org/10.1073/pnas.1019576108.
West, G.B., Brown, J.H., Enquist, B.J., 1999. A general model for the structure and allometry of plant vascular systems. Nature 400, 664–667. https://doi.org/10.1038/23251.
Zianis, D., Mencuccini, M., 2004. On simplifying allometric analyses of forest biomass. For. Ecol. Manage 187, 311–332. https://doi.org/10.1016/j.foreco.2003.07.007.